SLIRP mediates nuclear-mitochondrial communication during antiviral signaling to promote robust interferon response

Doyeong Ku[1], Yewon Yang[1], Youngran Park[2,3], Daesong Jang[4], Keonyong Lee[1], Namseok Lee[1], Yong-ki Lee[1], Jaeseon Lee[5], Yeon Bi Han[6], Soojin Jang[5], Se Rim Choi[7], You-Jung Ha[7], Yong Seok Choi[8], Woo-Jin Jeong[9,10], Yun Jong Lee[6,7], Kyung Jin Lee[5], Seunghee Cha[4,*], and Yoosik Kim[1,11,12,13,*]

[1]Department of Chemical and Biomolecular Engineering, Korea Advanced Institute of Science and Technology (KAIST), Daejeon, 34141, Republic of Korea
[2]Center for RNA Research, Institute of Basic Science, Seoul, 08826, Republic of Korea
[3]School of Biological Sciences, Seoul National University, Seoul, 08826, Republic of Korea
[4]Department of Oral and Maxillofacial Diagnostic Science, Center for Orphaned Autoimmune Disorders, University of Florida College of Dentistry, Gainesville, Florida, 32610, United States of America
[5]R&D Institute, ORGANOIDSCIENCES Ltd., Seongnam, 13488, Republic of Korea
[6]Department of Pathology and Translational Medicine, Seoul National University Bundang Hospital, Seongnam, 13620, Republic of Korea
[7]Division of Rheumatology, Department of Internal Medicine, Seoul National University Bundang Hospital, Sengonam, 13620, Republic of Korea
[8]Medical Science Research Institute, Seoul National University Bundang Hospital, Sengonam, 13620, Republic of Korea
[9]Department of Otorhinolaryngology - Head & Neck Surgery, Seoul National University Bundang Hospital, Sengonam, 13620, Republic of Korea
[10]Sensory Organ Research Institute, Seoul National University Medical Research Center, Seoul National University College of Medicine, Seoul, Republic of Korea
[11]Graduate School of Engineering Biology, KAIST, Daejeon, 34141, Republic of Korea
[12]KAIST Institute for BioCentury (KIB), Daejeon, 34141, Republic of Korea
[13]KAIST Institute for Health Science and Technology (KIHST), Daejeon 34141, Republic of Korea

* To whom correspondence should be addressed. Yoosik Kim, Tel) +82-42-350-7312, Fax) +82-42-350-3910, Email) ysyoosik@kaist.ac.kr. Seunghee Cha, Tel) +1-352-273-6687, Fax) +1-352-294-8064, Email) scha@dental.ufl.edu

ABSTRACT

Viral and endogenous double-stranded RNAs (dsRNAs) are recognized by cytosolic sensors and initiate antiviral signaling as a part of innate responses. Recent studies reveal a close association between mitochondrial dsRNAs (mt-dsRNAs) and several immune-related diseases. However, the mechanism by which mt-dsRNAs stimulate immune responses remains poorly understood. Here, we discover SRA stem-loop interacting RNA binding protein (SLIRP) as a key amplifier of mt-dsRNA-triggered antiviral signals in the setting of an autoimmune condition and viral infection. We find that the activation of melanoma differentiation-associated gene 5 (MDA5) by dsRNAs upregulates SLIRP expression and facilitates its mitochondrial import. SLIRP then stabilizes mt-dsRNAs and promotes their cytosolic release where they further activate MDA5 to amplify the antiviral signaling, augmenting the interferon response. Interestingly, downregulation of cytosolic mt-dsRNAs by targeted knockdown of SLIRP or blocking mt-dsRNA release from mitochondria dampens the interferon response and increases cell vulnerability to certain viral infections. Furthermore, we find elevated SLIRP expression in monocytes of autoimmune patients, and downregulation of SLIRP partially rescues the abnormal interferon-stimulated gene expression in patients' primary cells. Our study unveils amplified positive feedback of antiviral signaling through the stabilization of mt-dsRNAs by SLIRP, which promotes a robust interferon response.

KEYWORDS

Double-stranded RNAs, antiviral signaling, mitochondrial RNAs, SLIRP, interferon response, autoimmune disease, viral infection, mitochondrial-nuclear communication

Supplemental material is available for this article.

INTRODUCTION

Long double-stranded RNAs (dsRNAs) are generally produced during viral replication and are considered a signature of infection (Ehrenfeld and Hunt 1971; Weber et al. 2006). These molecules act as pathogen-associated molecular patterns (PAMPs) and are recognized by dsRNA-specific pattern recognition receptors (PRRs), such as Toll-like receptor 3 (TLR3) (Alexopoulou et al. 2001), retinoic acid-inducible gene-I (RIG-I), melanoma differentiation-associated gene 5 (MDA5) (Rehwinkel and Gack 2020), and protein kinase R (PKR) (Dey et al. 2005). When activated by dsRNAs, these sensors trigger the expression of type I interferon (IFN) and IFN-stimulated genes (ISGs) to interfere with viral replication and suppress global translation to induce apoptosis of infected cells (Peisley and Hur 2013; Hur 2019).

The innate immune response can be activated by endogenous dsRNAs that are naturally present in our cells (Kim et al. 2019b). Due to their immunogenic potential, the expression and recognition of dsRNAs are strictly regulated. The dsRNAs encoded by the nuclear genome are mostly suppressed through epigenetic modification (Chen and Hur 2022). When transcribed, these RNAs are often edited by adenosine deaminase acting on RNA (ADAR), which disrupts the secondary structure to avoid recognition by dsRNA sensors (Athanasiadis et al. 2004; Kim et al. 2004; Levanon et al. 2004; Peng et al. 2012; Quin et al. 2021). More recently, studies showed that cells express circular RNAs with short hairpin structures to prevent activation of PKR (Chen et al. 2017; Liu et al. 2019). However, our understanding of the regulation of mitochondrial dsRNAs (mt-dsRNAs) is highly limited.

mt-dsRNAs are generated due to bidirectional transcription of the mitochondrial circular genome (Anderson et al. 1981; D'Souza and Minczuk 2018), which produces long complementary RNAs denoted as heavy and light strand RNAs (Aloni and Attardi 1971; Harel et al. 1975; Murphy et al. 1975; Young and Attardi 1975; Ojala et al. 1981; Peng et al. 2012; Dhir et al. 2018). Under stress conditions, mt-dsRNAs are released to the cytosol through BCL-2-associated X protein (BAX)/BCL-2-homologous antagonist/killer (BAK1) channel (Youle and Strasser 2008; White et al. 2014; Dhir et al. 2018) where they activate MDA5 and PKR to initiate IFN response and apoptosis (Dhir et al. 2018; Kim et al. 2018). To limit mt-dsRNA expression, light strand mtRNAs are degraded by mtRNA degradosome complex consisting of human suppressor of var1,3-like (hSUV3) (Szczesny et al. 2010) and polyribonucleotide nucleotidyltransferase 1 (PNPT1) (Chen et al. 2006; Wang et al. 2010; Borowski et al. 2013).

Recently, studies reported misregulation of mt-dsRNAs in diseases that accompany aberrant immune activation, such as osteoarthritis (OA) (Kim et al. 2022), Huntington's disease

(Lee et al. 2020a), alcohol-associated liver disease (Lee et al. 2020b), and autoimmune Sjögren's disease (SjD) (Yoon et al. 2022). In particular, mt-dsRNAs are upregulated in saliva, tear, and primary salivary gland epithelial cells of SjD patients as well as in the mouse model of SjD (Yoon et al. 2022). Moreover, mt-dsRNA levels are also elevated in the chondrocytes and synovial fluids of OA patients (Kim et al. 2022). Notably, the upregulation of mtRNA expression is not limited to these inflammatory diseases. In response to various viral infections, such as respiratory syncytial virus (RSV), severe acute respiratory syndrome coronavirus (SARS-CoV), and SARS-CoV-2 (Shao et al. 2006; Miller et al. 2021), mtRNA levels in the infected cells are elevated, suggesting a potential role of mtRNA upregulation in regulating antiviral signaling. Indeed, reducing mtRNA expression decreased the IFN response to exogenous dsRNAs and alleviated glandular phenotypes of SjD (Yoon et al. 2022). Despite the general occurrence of mtRNA upregulation and its regulatory potential on antiviral response, the underlying mechanism of mtRNA regulation remains unknown.

In this study, we investigated the regulatory mechanism and biological significance of mt-dsRNA regulation during antiviral signaling. By screening the genes involved in mtRNA stability, we found that mt-dsRNA upregulation is mediated by SRA stem-loop interacting RNA binding protein (SLIRP) that enhances mtRNA stability. We further analyzed the SLIRP expression, localization, and interaction with mtRNAs to elucidate the molecular process behind mtRNA upregulation. We further examined the clinical implications by investigating the role of SLIRP in the context of viral infection and autoimmune diseases, such as systemic lupus erythematosus (SLE) and SjD. Collectively, our study establishes SLIRP as an essential mediator of nuclear-mitochondrial communication during antiviral signaling and a potential target to alleviate aberrant immune activation.

RESULTS

mtRNA expression is upregulated during antiviral signaling

We have previously shown that mtRNA expression is strongly induced by antiviral signaling to exogenous dsRNAs (Yoon et al. 2022) and mitochondrial stressors like oligomycin A and hydrogen peroxide (Kim et al. 2022). However, it remains unclear whether mtRNAs are always induced downstream of antiviral response or by other stressors. For example, mtRNAs were not induced under endoplasmic reticulum stress from increased misfolded proteins (Yoon et al. 2023). Thus, we began our investigation by specifying stressors that can potentially modulate mtRNA expression.

We obtained several representative innate immune stressors based on their well-known non-self signatures and interacting PRRs and evaluated their impact on mtRNA expression (Figure S1A). We used lipopolysaccharide (LPS) stimulating TLR4 as a non-nucleic acid PAMP, single-strand poly-uridine (ssPolyU) as an agonist of TLR7 and TLR8, 5′ triphosphate hairpin RNA (3p-hpRNA) as an agonist of RIG-I, and synthetic dsRNAs (short, long, and polyinosinic-polycyticylic acid, poly I:C) as agonists of RIG-I, MDA5, TLR3, and PKR. We also examined the DNA stressor, CpG oligodeoxynucleotides (CpG ODN), which can act as an agonist of cyclic GMP-AMP synthase (cGAS) and TLR9.

Among various non-self signatures, only long synthetic dsRNA transfection induced strong upregulation of both total mtRNAs and mt-dsRNAs (Figures 1A and 1B). Of note, mt-dsRNA expression was inferred by examining the individual expression of heavy and their complementary light strand mtRNAs via strand-specific reverse transcription (Kim et al. 2023). Transfection of short synthetic dsRNAs (79 bp duplex RNA with random sequences) increased the expression of light strand mtRNAs, with no notable alteration in the heavy strands and total mtRNAs. Meanwhile, transfection of long synthetic dsRNAs (717 bp duplex RNA derived from *EGFP* sequences) and poly I:C (average length of 1,000~1,800 bp) increased mtRNA expression from both strands. Interestingly, long synthetic dsRNAs and poly I:C yielded similar effects on mtRNAs, suggesting that the upregulation of mtRNAs is not dsRNA-sequence specific but rather a general downstream response to long dsRNA transfection.

In contrast to dsRNAs, LPS treatment did not cause a significant change in total mtRNA expression while ssPolyU treatment and 3p-hpRNA transfection even reduced total mtRNA expression (Figures S1B-D). Treatment with poly I:C to activate TLR3 resulted in a slight increase in total mtRNA expression with a large variance between biological replicates (Figure S1E). Lastly, neither treatment nor transfection of CpG ODN to activate TLR9 or cGAS, respectively, elicited any significant alterations in total mtRNA expression (Figures S1F and S1G).

As mtRNA induction occurred most strongly as a downstream response to long dsRNA transfection, we focused on poly I:C for the remainder of the study. Through single-molecular RNA fluorescent in situ hybridization (smRNA-FISH), we visualized and quantified the increased expression of *ND5* mtRNAs upon poly I:C transfection (Figure 1C). Of note, *ND5* was chosen as a representative mtRNA because *ND5* light and heavy strand mtRNAs showed strong induction in our previous studies (Kim et al. 2022; Yoon et al. 2022; Kim et al. 2023). To complement smRNA-FISH data, we performed RNA-seq analysis and found that both

strands of all examined mtRNAs, except for the light strand *ND6*, were upregulated upon poly I:C transfection (Figure 1D). Such upregulation of mtRNAs was consistently observed across multiple cell lines, such as A549 lung adenocarcinoma and PC3 prostatic adenocarcinoma, indicating that it might be a common downstream response to dsRNA-mediated antiviral response (Figures S1H and S1I). Along with the increased mtRNA expression, our transcriptomic analysis revealed increased expression of ISGs (Figure 1E), indicating the activation of antiviral signaling upon poly I:C. In line with this, cellular pathways related to antiviral signaling, including inflammatory response and defense response to a virus, were significantly activated (Figure 1F).

Considering that poly I:C is commonly used to mimic viral infection, we further investigated the expression of mtRNAs in cells infected with SARS-CoV-2 by reanalyzing publicly available RNA-seq data (Miller et al. 2021). Clearly, our analysis showed that mtRNAs derived from both heavy and light strand were upregulated in A549-ACE2 and Calu3 cells infected with SARS-Cov-2, underscoring the potential implications of mtRNA and mt-dsRNA regulation during antiviral signaling (Figures 1G and 1H). Collectively, our findings suggested that long dsRNA stressors specifically stimulate mtRNA upregulation.

SLIRP stabilizes mtRNAs during poly I:C stimulation

Next, we investigated the underlying mechanism for mtRNA upregulation during antiviral signaling. We hypothesized three possible mechanisms: increased mtDNA replication, mtRNA transcription, and mtRNA stability. First, we analyzed the mtDNA copy number in response to poly I:C stimulation using qPCR and gel electrophoresis and found no significant alteration (Figures 2A and 2B). We then examined the effect of mtRNA transcription by pre-treating cells with an inhibitor of mitochondrial transcription (inositol 4-methyltransferase (IMT1)) (Bonekamp et al. 2020) for 41 h before poly I:C transfection. Indeed, treating cells with IMT1 significantly decreased the mtRNA expression (Figure S2A). Yet, we still clearly observed increased expression of mtRNAs upon poly I:C transfection even when the mtRNA transcription was blocked (Figure 2C). Considering that the degree of induction between mock and IMT1-treated cells is similar, we ruled out the possibility of leaky transcription due to imperfect inhibition of mtRNA polymerase by IMT1. Of note, we normalized mtRNA expression prior to poly I:C transfection to focus on the degree of induction rather than the relative expression level of mtRNAs upon poly I:C transfection.

To test whether mtRNA stability was responsible for the increased mtRNA expression, we knocked down six key regulators known to be involved in stability individually and examined their impact on mtRNA induction. Previous studies have established that post-transcriptional regulation of mtRNAs is a balance between degradation by mitochondrial degradosome complex, consisting of RNA exonuclease 2 (REXO2) (Szewczyk et al. 2020), hSUV3 (Szczesny et al. 2010), and PNPT1 (Chen et al. 2006; Wang et al. 2010; Borowski et al. 2013) and stabilization by leucine-rich pentatricopeptide repeat-containing protein (LRPPRC) (Ruzzenente et al. 2012), SLIRP (Sasarman et al. 2010; Chujo et al. 2012; Lagouge et al. 2015), and mitochondrial poly(A) polymerase (mtPAP) (Nagaike et al. 2005). We used siRNAs to knock down these genes individually, transfected cells with poly I:C, and then examined the induction of mtRNAs. Again, to focus on the degree of induction, we normalized the mtRNA expression in cells deficient of the individual target gene without poly I:C transfection. Among these candidates, we found that SLIRP knockdown resulted in a significant decrease in the degree of all mtRNA induction by poly I:C (Figures 2D and S2B-F). More importantly, in SLIRP-deficient cells, the mtRNA induction was nearly completely abolished, indicating that SLIRP is the primary factor in upregulating mtRNA expression during antiviral response (Figure 2E). When we performed strand-specific RT-qPCR to examine the two strands of mt-dsRNAs independently, we found that the SLIRP knockdown decreased induction in both strands, with a stronger effect on the heavy strand mtRNAs (Figure 2F).

SLIRP expression and its mitochondrial localization are affected by poly I:C

SLIRP is a mtRNA binding protein that interacts with stem-loop structures in the 3′ untranslated regions to protect the RNA from decay (Sasarman et al. 2010; Chujo et al. 2012; Lagouge et al. 2015). Our data suggests a model where the RNA stabilizing effect of SLIRP is enhanced during antiviral response and results in increased mtRNA levels. Consistent with our model, we found about a 50% increase in both mRNA and protein expression of SLIRP in poly I:C-transfected cells (Figures 3A and 3B). When we examined the SLIRP subcellular localization, we found increased SLIRP expression in the membrane fraction, which contains membrane organelles, including mitochondria (Figure 3C). Indeed, SLIRP showed a higher degree of colocalization with the mitochondria in immunocytochemistry (Figure 3D).

For more direct confirmation, we employed formaldehyde crosslinking and immunoprecipitation (fCLIP) and examined SLIRP-mtRNA interactions (Figure S3A). In cells

transfected with poly I:C, SLIRP was more strongly bound to mtRNAs, except for *ND5*, which showed large variability (Figure 3E). Moreover, we analyzed the effect of mtRNA stability in SLIRP-deficient cells after blocking mtRNA transcription using IMT1 (Bonekamp et al. 2020). As a control, we examined the stability of six mtRNA genes in siLuc-transfected cells before and after poly I:C transfection. Consistent with our earlier data, we found a dramatic increase in mtRNA stability in poly I:C transfected cells (Figures 3F and S3B). Interestingly, we no longer observed increased mtRNA stability by poly I:C in SLIRP-deficient cells (Figures 3F and S3B). There was a slight increase in mtRNA levels in 2 h sample, but the magnitude was minor compared to that of the control (siLuc) cells.

We further investigated the mechanism responsible for increased SLIRP localization to mitochondria during antiviral response to poly I:C. To this end, we examined the role of translocase of the outer membrane (TOM) complex, which plays a crucial role in recognizing mitochondrial targeting signals to facilitate the entry of precursor proteins into the mitochondria (Wiedemann and Pfanner 2017; Araiso et al. 2022; Sayyed and Mahalakshmi 2022). The key components of the TOM complex include translocase of outer mitochondrial membrane 20 (TOMM20) and TOMM22 (Yamano et al. 2008; Su et al. 2022a), the central channel protein, TOMM40 (Ahting et al. 2001), and an accessory protein TOMM70 (Kreimendahl and Rassow 2020). We examined the effect of poly I:C transfection on their mRNA expression and found increased expression in all except for *TOMM22* (Figure 3G). We then applied a similar approach as above and knocked down these four *TOMM* genes individually and examined their effects on mtRNA induction by poly I:C. Remarkably, our mini-screening revealed that knockdown of TOMM40, an essential component of TOM complex forming the main channel pore (Ahting et al. 2001), resulted in decreased induction of mtRNAs upon poly I:C stimulation, except for *CO3* (Figure 3H and S4A-D). To test whether the knockdown of TOMM40 affected SLIRP localization, we performed subcellular fractionation and examined SLIRP expression in TOMM40-deficient cells transfected with poly I:C. While control cells showed increased SLIRP localization to the membrane fraction upon poly I:C transfection, in TOMM40-deficient cells, SLIRP recruitment to the membrane fraction was not facilitated (Figure 3I). Together, these data indicate that the increased expression and enhanced mitochondrial import of SLIRP by the mitochondrial protein import system, particularly TOMM40, plays a pivotal role in the induction of mtRNA via increased stability during antiviral response.

SLIRP-mtRNA-MDA5 positive feedback loop amplifies antiviral signaling

One key downstream effect of mtRNA upregulation is that mt-dsRNA level is also increased, and when released to the cytosol, they can interact with PKR and MDA5 to activate antiviral signaling and induce type I IFN response (Dhir et al. 2018; Kim et al. 2022). Moreover, this mtRNA-mediated immune activation is closely associated with the development of autoimmune and inflammatory diseases (Lee et al. 2020a; Lee et al. 2020b; Kim et al. 2022; Yoon et al. 2022). Therefore, we asked whether SLIRP can affect the IFN response to exogenous dsRNAs by stabilizing and elevating mtRNA expression.

First, we examined IFN and ISG expression in cells deficient in SLIRP. According to our working model, with decreased expression of SLIRP, mtRNA expression is no longer elevated by poly I:C, which should result in decreased IFN response. Indeed, we found that SLIRP downregulation resulted in a significant reduction of IFN and ISG expression upon poly I:C transfection (Figure 4A). Of note, IFN and ISG expression are still induced by the introduction of poly I:C. However, in SLIRP knocked down cells, the degree of IFN and ISG induction was significantly decreased compared to the control cells. To further investigate whether this effect on ISG induction by SLIRP is mediated by mtRNAs, we examined the cytosolic release of mtRNAs. We found that SLIRP-deficient cells showed reduced cytosolic levels for most mtRNAs in response to poly I:C (Figure S5A and 4B). Together, these results indicate that mtRNA stabilization by SLIRP results in increased cytosolic release of mtRNAs during antiviral signaling to promote stronger IFN response.

We further characterized the importance of mtRNA release during antiviral signaling. Since mtRNAs and mt-dsRNAs are released to the cytosol through BAX/BAK micropores (Youle and Strasser 2008; White et al. 2014; Dhir et al. 2018), we downregulated BAK1 to hinder the cytosolic release of mtRNAs and examined the expression of selected ISGs. All examined ISGs showed decreased expression in BAK1 knocked down cells (Figure 4C). To our surprise, we found that the induction of most mtRNAs upon poly I:C stimulation was also significantly reduced in BAK1-deficient cells (Figure 4D), indicating that the cytosolic release of mtRNAs might contribute to upregulation of their own expression. This creates a positive feedback loop where activation of antiviral signaling by exogenous dsRNAs upregulates SLIRP and facilitates the mitochondrial import of SLIRP, where it stabilizes mtRNAs, which are then released to the cytosol to amplify the antiviral signaling further.

A missing component in our proposed feedback regulation is the factor that mediates SLIRP and mtRNA induction upon poly I:C transfection. To test, we downregulated the

dsRNA sensors individually and examined their effect on mtRNA levels. Only MDA5 knockdown resulted in a significantly reduced induction of mtRNAs upon poly I:C transfection (Figures 4E and S5B-D). In the presence of long dsRNAs, MDA5 forms a filament along the dsRNA, recruits mitochondrial antiviral signaling protein, and phosphorylates interferon regulatory factor 3 (IRF3) to trigger the IFN-β signaling pathway (Seth et al. 2005). Indeed, treating cells with IFN-β was sufficient in upregulating mtRNA expression even without poly I:C (Figure 4F). Moreover, in MDA5-deficient cells, SLIRP localization to mitochondria was no longer enhanced while control cells clearly showed increased SLIRP in the membrane fraction (Figure 4G). This suggests that MDA5 and the downstream IFN-β signaling are responsible for the mtRNA induction during antiviral response by recruiting SLIRP to mitochondria.

MDA5 is one of the ISGs and upregulates its own expression during antiviral response. Considering that SLIRP affects the global induction of ISGs during dsRNA stress, we examined whether MDA5 expression is under the control of SLIRP. Interestingly, we found that SLIRP knockdown results in decreased *MDA5* mRNA and protein expression (Figures 4H and 4I). The decreased MDA5 expression eventually resulted in reduced antiviral signaling, as the phosphor-IRF3 (pIRF3) was significantly reduced in SLIRP knocked down cells (Figure 4J). Collectively, we establish a positive feedback model of antiviral signaling consisting of MDA5 activation, enhanced SLIRP mitochondrial localization, stabilization and cytosolic release of mtRNAs and mt-dsRNAs, and further activation of MDA5 (Figure 4K).

SLIRP mediates cellular defense against human coronavirus OC43

One potential biological function of SLIRP-mediated mtRNA stabilization is cellular defense against viral infection. Specifically, our positive feedback loop model implies that SLIRP may be required for a robust IFN response to viral infection to hinder or arrest viral replication. To test this hypothesis, we knocked down SLIRP in A549 cells using shRNAs and infected cells with human coronavirus OC43 or human influenza A virus (A/Puerto Rico/8/1934(H1N1), PR8) (Figure 5A). OC43 is a positive-strand RNA virus known to produce dsRNAs in cells during viral replication (Matoba et al. 2015), whereas PR8 is a negative-strand RNA virus with low dsRNA generation (Weber et al. 2006). We found that the viral mRNA expression of OC43 was significantly increased in SLIRP-deficient cells, indicating enhanced viral replication (Figure 5B). Interestingly, despite the increased viral replication, the expression of *IFN-β* and selected ISGs was lower, indicating impaired innate

immune response in SLIRP-deficient cells (Figure 5C). When we performed a similar experiment for the PR8 virus, SLIRP downregulation decreased the level of viral mRNA (Figure S6A). In addition, the ISG expression was unaffected in SLIRP-deficient cells infected with the PR8 virus (Figure S6B).

To extend our findings to the SARS-CoV-2 virus, a positive-strand RNA virus, we infected Calu3 and A549-ACE2 cells with the SARS-CoV-2 virus and examined the effect of SLIRP downregulation on viral replication. We first confirmed the knockdown efficiency of SLIRP in Calu3 via western blotting (Figure S6C). We then infected Calu3 cells with SARS-CoV-2 at MOI of 1 and 0.1, but found that SLIRP downregulation did not affect viral mRNA expression (Figure S6D). The expression of *IFN-β* and *TLR3* was even increased upon SARS-CoV-2 infection in cells deficient in SLIRP (Figure S6E). Next, we used A549-ACE2 as a different cell line susceptible to SARS-CoV-2 infection. Again, we began by confirming the degree of SLIRP knockdown by shSLIRP in A549-ACE2 cells (Figure S6F) and infected cells with SARS-CoV-2 virus at MOI of 1 and 0.1. However, for A549-ACE2, SLIRP downregulation decreased viral mRNA expression (Figure S6G). Moreover, SLIRP downregulation did not affect the expression of *TLR3* and *IFI27* while the expression of *IFN-β* and *CXCL10* was increased (Figure S6H).

SLIRP is upregulated in autoimmune patients and may drive abnormal IFN signature

We have previously shown that mtRNAs are upregulated in patients with systemic autoimmune diseases, such as SjD (Yoon et al. 2022). Moreover, abnormal activation of PRRs and subsequent misactivation of antiviral signaling are representative signatures of SjD (Deshmukh et al. 2009; Nandula et al. 2011; Shimizu et al. 2021) and SLE (Hooks et al. 1979; Ronnblom and Pascual 2008). Based on the findings of the current study, we investigated the potential involvement of SLIRP in the elevation of mtRNAs observed in autoimmune patients. First, we reanalyzed previously published bulk RNA-seq data of SjD and SLE patients (Lee et al. 2022). To determine differentially expressed genes (DEGs), gene expression in CD14+ monocytes isolated from whole blood of SjD and SLE patients (females, ages 32 to 62) were compared to those from healthy controls (HCs) monocytes (females, ages 30 and 33). Interestingly, we found a significant increase in *SLIRP* mRNA expression in both SjD and SLE patients (Figure 6A), suggesting the potential association between *SLIRP* and these autoimmune diseases. At the same time, the expression of other post-transcriptional regulators of mtRNAs, such as *LRPPRC*, *REXO2*, and *hSUV3*, did not show significant differences. Of

note, SjD patients exhibited a significantly elevated expression of *PNPT1*, a component of mtRNA degradosome, and SLE patients showed decreased expression of *mtPAP*, a poly(A) polymerase of mtRNAs. However, since the upregulation of these genes should lead to mt-dsRNA degradation, it cannot account for the observed increased mtRNA expression.

Next, we investigated the upregulation of SLIRP in different types of SjD. We obtained and analyzed monocytes from SjD patients of varying ages, including five adults (SjD) and four children diagnosed with SjD (cSjD) as well as monocytes from various control groups: five HCs (mostly young adults), four symptomatic pediatric patients who do not meet the criteria for cSjD diagnosis (Non-cSjD), and six non-cSjD patients with the potential to develop SjD in the future based on their positive lip biopsy results (BxP). Our transcriptome analysis revealed an overall increase in *SLIRP* mRNA expression in SjD patients, except for one patient, compared to the control groups, indicating a potential association between *SLIRP* and SjD. Two cSjD patients also showed increased SLIRP expression, while the others did not. In contrast, genes responsible for stabilizing mtRNAs, such as *LRPPRC* and *mtPAP*, did not show significant changes in their expression among SjD patients and control groups (Figure 6B). When we examined mtRNA degradosome components, *PNPT1* was significantly increased in SjD patients, which works against our findings of increased mtRNA expression (Figure 6C). The expression of other genes related to mtRNA degradosome in SjD and cSjD was indistinguishable from those of the control groups (Figure 6C).

We further investigate the role of SLIRP in aberrant IFN signatures in SjD by analyzing the primary cells derived from patients' minor salivary gland lip biopsy specimens. We first characterized the IFN signature and found that two patients (P1 and P2) exhibited elevated expression of *IFN-β* and several ISGs related to SjD, whereas their downregulation was noted in P3 (Figure 6D). Interestingly, the further downregulation of SLIRP with siRNA resulted in reduced *IFN-β* and some ISG expression in both P1 and P2 (Figures 6E and 6F) despite the large variations. On the other hand, SLIRP downregulation in P3 increased *IFN-β* and ISG expression (Figure 6G).

DISCUSSION

Our study establishes the positive feedback regulatory mechanism of mt-dsRNAs during antiviral signaling through stabilization by SLIRP. According to our model, activation of MDA5 by dsRNAs and downstream IFN response upregulates SLIRP and facilitates SLIRP localization to mitochondria through the mitochondrial import system, especially TOMM40.

Inside mitochondria, SLIRP stabilizes mtRNAs to elevate their expression. The increased mtRNAs are then released to the cytosol via BAX/BAK micropores, where they are recognized by PRRs, including MDA5, and activate MDA5. This positive feedback amplification of antiviral signaling by SLIRP and mtRNAs results in a robust IFN response to exogenous dsRNAs. Moreover, our study suggests SLIRP as a putative regulator of aberrant antiviral signatures found in autoimmune patients and a key defense molecule against viruses, including OC43.

Numerous previous studies showed the association of mt-dsRNAs with aberrant immune activation during the development of inflammatory and autoimmune diseases (Lee et al. 2020a; Lee et al. 2020b; Kim et al. 2022; Yoon et al. 2022). Moreover, mt-dsRNAs can be released to the cytosol during oxidative stress and mitochondrial dysfunction as well as in response to DNA damage and activate PKR to initiate apoptotic programs (Kim et al. 2018; Kim et al. 2022). In the current study, we focused on mt-dsRNA induction during antiviral response and identified key components, such as SLIRP, TOMM40, and MDA5, that are required for mtRNA induction and subsequent amplification of the IFN response. Consistent with our results, a recent proteomics study identified TOMM40 as one of six consistently upregulated proteins in SLE patients (Li et al. 2022). In the future, it would be interesting to study whether SLIRP is also involved in other stress conditions where mt-dsRNAs activate the cytosolic dsRNAs sensors.

Our study attempted to address the biological significance behind the SLIRP-mediated amplification of the antiviral response in the context of autoimmune disease and viral infection. The upregulation of SLIRP in the monocytes of SjD and SLE, together with the upregulation of mtRNAs, suggest a potential role of SLIRP in the development of autoimmune disease. Indeed, the elevation of mtRNAs is associated with the pathogenesis of SjD, while SLE patients produce auto-antibodies that recognize mtRNAs (Pan et al. 2020). In addition, the abnormal activation of PRRs and antiviral signaling are well-known signatures of autoimmune diseases (Hooks et al. 1979; Ronnblom and Pascual 2008; Deshmukh et al. 2009; Nandula et al. 2011; Shimizu et al. 2021). Moreover, our study suggests SLIRP as a potential target to alleviate the upregulation of IFN signature in autoimmune patients, as downregulation of SLIRP in the primary minor salivary gland cells of SjD patients resulted in a moderate reduction in the expression of selected ISGs. Yet, one of the patient cells with the lowest ISG expression showed no further decrease in ISG mRNA levels upon SLIRP knockdown. One possibility is that targeting SLIRP might provide benefits to patients with high ISG signatures. Although the

number of patients is too few (due to the difficult nature of obtaining samples of rare cSjD disease patient samples) to make a conclusive remark, our findings suggest a potential for downregulating SLIRP to attenuate abnormal IFN signatures in SjD patients that exhibited elevated IFN and ISG expression. Future investigation using additional patients with various ISG expression patterns may provide a specific patient group where SLIRP downregulation may alleviate aberrant ISG expression.

One limitation of our study is that we used poly I:C to trigger antiviral signaling. Although poly I:C is commonly used to mimic viral infection as long dsRNAs are generated as byproducts of viral replication, viruses develop multiple mechanisms to avoid dsRNA sensing inside the cell (van de Sandt et al. 2012; Deng et al. 2017; Kasuga et al. 2021; Minkoff and tenOever 2023). For example, certain viruses form a specific replication compartment within the cytosol to shield the viral dsRNAs from PRRs (Kasuga et al. 2021). The *Flaviviridae* family of influenza viruses can replicate in the nucleus to avoid cytosolic PRRs (De Jesus-Gonzalez et al. 2021). Moreover, morbillivirus in the *Paramyxoviridae* family post-translationally modify MDA5 to prevent its activation (Goodbourn and Randall 2009). Similarly, SARS-CoV-2 encodes ORF3c protein that blocks MDA5 activation (Stewart et al. 2023). Perhaps, these strategies allow viruses to avoid SLIRP-mediated amplification of antiviral response. Of note, in our study, knockdown of SLIRP resulted in decreased viral replication for PR8 and SARS-CoV-2, but we believe that this reflects decreased proliferation in SLIRP knocked down cells instead of its effect on antiviral signaling. At the same time, in the case of OC43 human coronavirus, knockdown of SLIRP resulted in decreased antiviral signaling while viral replication was enhanced. These results suggest that MDA5-SLIRP-mtRNA feedback regulation of antiviral signaling might have been developed as a mechanism for cellular defense against viruses. In this context, mitochondria, products of endosymbiosis, are working together with the host genomic factor (SLIRP) to provide immunogenic materials (mt-dsRNAs) to defend the host cell against foreign threats (viruses). It remains to be investigated how viruses evolved to avoid PRR recognition and prevent the initiation of the positive feedback loop.

In summary, our study underscores the nuclear-mitochondrial communication during antiviral signaling that utilizes mitochondrial immunogenic materials as a snowball for robust immune response. Detailed analysis of the mechanism and application of such regulation of mtRNAs by SLIRP and MDA5 will enhance our understanding of aberrant immune signatures in autoimmune diseases and host defense against viruses.

MATERIAL AND METHODS

Cell culture

All cells were grown in the proper condition descibed in the Supplemental Material. For human salivary gland primary cells, the published protocol (Su et al. 2022b) was used with a minor modification. The biopsy tissues were obtained from patients at the Center for Orphaned Autoimmune Disorders at the University of Florida College of Dentistry. The informed consent form was signed by each participant according to the protocol (#IRB201900645) approved by the UF Institutional Review Board.

Transfection

Various agonists were transfected into cells to stimulate cytosolic PRRs described in the Supplemental Material. Short synthetic dsRNAs with random sequences and a length of 79 base pairs (bp) were prepared as described in a previous study from the Bevilacqua group (Zheng and Bevilacqua 2004). Long synthetic dsRNAs were synthesized by in vitro transcribing the *EGFP* gene (717 bp) in sense and antisense direction and annealing the two complementary RNAs, as explained in a previous study from our group (Kang et al. 2022). Sequences of the siRNAs used in this study are provided in Table S1.

RNA isolation and RT-qPCR

Cellular RNAs were isolated and quantified as described in Supplemental Materials. Primers used in this study are provided in Table S2-S4.

Statistical and functional analysis of mRNA-seq data

For the analysis of RNA-seq data, sequencing read files were quality-checked with FastQC (version 0.11.9) for any abnormalities. Reads were aligned against the reference human genome (GRCh38) with STAR aligner (version 2.7.9) (Dobin et al. 2013). Gene quantification was performed simultaneously by providing --quantMode GeneCounts option. Reads were quantified against GENCODE human genome annotation (version 38) (Frankish et al. 2023). Differential gene expression analysis and other statistical calculations were performed using the DESeq2 package in R (Love et al. 2014).

For the analysis of RNA-seq data for SARS-CoV2-infected cells and organoids obtained from SjD patients, raw reads were mapped to the reference human genome (GRCh38) using HISAT2 v.2.1.0 using default parameters (Kim et al. 2019a). Uniquely and concordantly mapped reads were selected using samtools and then quantified against the GENCODE human genome (version 34) using featureCounts. Differential gene expression analysis and other statistical calculations were performed using the DESeq2 package in R.

Other detailed experimental procedures are described in the Supplemental Material.

Data deposition

All data needed to evaluate the conclusions in the paper are present in the paper and/or the Supplementary Data. Further information and requests for resources and reagents should be directed to and will be fulfilled by the corresponding authors. Sequencing and processed data files of HCT116 cells upon poly I:C transfection were available at the Gene Expression Omnibus (GEO; https://www.ncbi.nlm.nih.gov/geo/) repository, with GEO accession GSE248259.

COMPETING INTEREST STATEMENT

Jaeson Lee, Soojin Jang, and Kyung Jin Lee are employees of ORGANOIDSCIENCES Ltd. Other authors have no conflict of interest to declare.

ACKNOWLEDGEMENTS

The authors thank all members of the Cha and Kim laboratories for their helpful discussions and comments on the paper. We thank Dr. V. Narry Kim from Seoul Naitional University for providing Calu3 cells and insightful suggestions on the study. This work was supported by the Ministry of Health & Welfare grant number HI21C1501.

AUTHOR CONTRIBUTIONS: D.K., S.C., and Y.K. conceived and designed the study. D.K. conducted most of the experiments. Y.Y performed experiments from figure S4. Y.P. performed SARS-CoV-2 experiments. D.J. prepared patient's monocytes and primary cells. K.L. and N.L. performed the bioinformatics analyses. Y.L. prepared OC43 virus experiments. J.L., Y.H., S.J., S.C., Y.H., Y.C., W.J., Y.L., and K.L. prepared patient's samples. D.K., Y.Y., and Y.K. analyzed data, interpreted the results, and generated the figures. D.K., Y.P., D.J., Y.K.

wrote the original draft. D.K., Y.Y., Y.L., V.K., K.L., S.C., and Y.K. reviewed and edited the manuscript. S.C. and Y.K. supervised the study.

REFERENCES

Ahting U, Thieffry M, Engelhardt H, Hegerl R, Neupert W, Nussberger S. 2001. Tom40, the pore-forming component of the protein-conducting TOM channel in the outer membrane of mitochondria. J Cell Biol 153: 1151-1160.

Alexopoulou L, Holt AC, Medzhitov R, Flavell RA. 2001. Recognition of double-stranded RNA and activation of NF-kappaB by Toll-like receptor 3. Nature 413: 732-738.

Aloni Y, Attardi G. 1971. Symmetrical in vivo transcription of mitochondrial DNA in HeLa cells. Proc Natl Acad Sci U S A 68: 1757-1761.

Anderson S, Bankier AT, Barrell BG, de Bruijn MH, Coulson AR, Drouin J, Eperon IC, Nierlich DP, Roe BA, Sanger F et al. 1981. Sequence and organization of the human mitochondrial genome. Nature 290: 457-465.

Araiso Y, Imai K, Endo T. 2022. Role of the TOM Complex in Protein Import into Mitochondria: Structural Views. Annu Rev Biochem 91: 679-703.

Athanasiadis A, Rich A, Maas S. 2004. Widespread A-to-I RNA editing of Alu-containing mRNAs in the human transcriptome. PLoS Biol 2: e391.

Bonekamp NA, Peter B, Hillen HS, Felser A, Bergbrede T, Choidas A, Horn M, Unger A, Di Lucrezia R, Atanassov I et al. 2020. Small-molecule inhibitors of human mitochondrial DNA transcription. Nature 588: 712-716.

Borowski LS, Dziembowski A, Hejnowicz MS, Stepien PP, Szczesny RJ. 2013. Human mitochondrial RNA decay mediated by PNPase-hSuv3 complex takes place in distinct foci. Nucleic Acids Res 41: 1223-1240.

Chen HW, Rainey RN, Balatoni CE, Dawson DW, Troke JJ, Wasiak S, Hong JS, McBride HM, Koehler CM, Teitell MA, French SW. 2006. Mammalian polynucleotide phosphorylase is an intermembrane space RNase that maintains mitochondrial homeostasis. Mol Cell Biol 26: 8475-8487.

Chen YG, Hur S. 2022. Cellular origins of dsRNA, their recognition and consequences. Nat Rev Mol Cell Biol 23: 286-301.

Chen YG, Kim MV, Chen X, Batista PJ, Aoyama S, Wilusz JE, Iwasaki A, Chang HY. 2017. Sensing Self and Foreign Circular RNAs by Intron Identity. Mol Cell 67: 228-238 e225.

Chujo T, Ohira T, Sakaguchi Y, Goshima N, Nomura N, Nagao A, Suzuki T. 2012. LRPPRC/SLIRP suppresses PNPase-mediated mRNA decay and promotes polyadenylation in human mitochondria. Nucleic Acids Res 40: 8033-8047.

D'Souza AR, Minczuk M. 2018. Mitochondrial transcription and translation: overview. Essays Biochem 62: 309-320.

De Jesus-Gonzalez LA, Palacios-Rapalo S, Reyes-Ruiz JM, Osuna-Ramos JF, Cordero-Rivera CD, Farfan-Morales CN, Gutierrez-Escolano AL, Del Angel RM. 2021. The Nuclear Pore Complex Is a Key Target of Viral Proteases to Promote Viral Replication. Viruses 13.

Deng X, Hackbart M, Mettelman RC, O'Brien A, Mielech AM, Yi G, Kao CC, Baker SC. 2017. Coronavirus nonstructural protein 15 mediates evasion of dsRNA sensors and limits apoptosis in macrophages. Proc Natl Acad Sci U S A 114: E4251-E4260.

Deshmukh US, Nandula SR, Thimmalapura PR, Scindia YM, Bagavant H. 2009. Activation of innate immune responses through Toll-like receptor 3 causes a rapid loss of salivary gland function. J Oral Pathol Med 38: 42-47.
Dey M, Cao C, Dar AC, Tamura T, Ozato K, Sicheri F, Dever TE. 2005. Mechanistic link between PKR dimerization, autophosphorylation, and eIF2alpha substrate recognition. Cell 122: 901-913.
Dhir A, Dhir S, Borowski LS, Jimenez L, Teitell M, Rotig A, Crow YJ, Rice GI, Duffy D, Tamby C et al. 2018. Mitochondrial double-stranded RNA triggers antiviral signalling in humans. Nature 560: 238-242.
Dobin A, Davis CA, Schlesinger F, Drenkow J, Zaleski C, Jha S, Batut P, Chaisson M, Gingeras TR. 2013. STAR: ultrafast universal RNA-seq aligner. Bioinformatics 29: 15-21.
Ehrenfeld E, Hunt T. 1971. Double-stranded poliovirus RNA inhibits initiation of protein synthesis by reticulocyte lysates. Proc Natl Acad Sci U S A 68: 1075-1078.
Frankish A, Carbonell-Sala S, Diekhans M, Jungreis I, Loveland JE, Mudge JM, Sisu C, Wright JC, Arnan C, Barnes I et al. 2023. GENCODE: reference annotation for the human and mouse genomes in 2023. Nucleic Acids Res 51: D942-D949.
Goodbourn S, Randall RE. 2009. The regulation of type I interferon production by paramyxoviruses. J Interferon Cytokine Res 29: 539-547.
Harel L, Riou G, Montagnier L. 1975. Nuclear and mitochondrial origin of rat liver double-stranded RNA. Biochimie 57: 227-233.
Hooks JJ, Moutsopoulos HM, Geis SA, Stahl NI, Decker JL, Notkins AL. 1979. Immune interferon in the circulation of patients with autoimmune disease. N Engl J Med 301: 5-8.
Hur S. 2019. Double-Stranded RNA Sensors and Modulators in Innate Immunity. Annu Rev Immunol 37: 349-375.
Kang M, Kharbash R, Byun JM, Jeon J, Ali AA, Ku D, Yoon J, Ku Y, Sohn J, Lee SV et al. 2022. Double-stranded RNA induction asa potential dynamic biomarkerfor DNA-demethylating agents. Mol Ther Nucleic Acids 29: 370-383.
Kasuga Y, Zhu B, Jang KJ, Yoo JS. 2021. Innate immune sensing of coronavirus and viral evasion strategies. Exp Mol Med 53: 723-736.
Kim D, Paggi JM, Park C, Bennett C, Salzberg SL. 2019a. Graph-based genome alignment and genotyping with HISAT2 and HISAT-genotype. Nat Biotechnol 37: 907-915.
Kim DD, Kim TT, Walsh T, Kobayashi Y, Matise TC, Buyske S, Gabriel A. 2004. Widespread RNA editing of embedded alu elements in the human transcriptome. Genome Res 14: 1719-1725.
Kim S, Ku Y, Ku J, Kim Y. 2019b. Evidence of Aberrant Immune Response by Endogenous Double-Stranded RNAs: Attack from Within. Bioessays 41: e1900023.
Kim S, Lee K, Choi YS, Ku J, Kim H, Kharbash R, Yoon J, Lee YS, Kim JH, Lee YJ, Kim Y. 2022. Mitochondrial double-stranded RNAs govern the stress response in chondrocytes to promote osteoarthritis development. Cell Rep 40: 111178.
Kim S, Yoon J, Lee K, Kim Y. 2023. Analysis of mitochondrial double-stranded RNAs in human cells. STAR Protoc 4: 102007.
Kim Y, Park J, Kim S, Kim M, Kang MG, Kwak C, Kang M, Kim B, Rhee HW, Kim VN. 2018. PKR Senses Nuclear and Mitochondrial Signals by Interacting with Endogenous Double-Stranded RNAs. Mol Cell 71: 1051-1063 e1056.
Kreimendahl S, Rassow J. 2020. The Mitochondrial Outer Membrane Protein Tom70-Mediator in Protein Traffic, Membrane Contact Sites and Innate Immunity. Int J Mol Sci 21.

Lagouge M, Mourier A, Lee HJ, Spahr H, Wai T, Kukat C, Silva Ramos E, Motori E, Busch JD, Siira S et al. 2015. SLIRP Regulates the Rate of Mitochondrial Protein Synthesis and Protects LRPPRC from Degradation. PLoS Genet 11: e1005423.
Lee H, Fenster RJ, Pineda SS, Gibbs WS, Mohammadi S, Davila-Velderrain J, Garcia FJ, Therrien M, Novis HS, Gao F et al. 2020a. Cell Type-Specific Transcriptomics Reveals that Mutant Huntingtin Leads to Mitochondrial RNA Release and Neuronal Innate Immune Activation. Neuron 107: 891-908 e898.
Lee JH, Shim YR, Seo W, Kim MH, Choi WM, Kim HH, Kim YE, Yang K, Ryu T, Jeong JM et al. 2020b. Mitochondrial Double-Stranded RNA in Exosome Promotes Interleukin-17 Production Through Toll-Like Receptor 3 in Alcohol-associated Liver Injury. Hepatology 72: 609-625.
Lee KE, Mun S, Kim SM, Shin W, Jung W, Paek J, Lee J, Hudson E, Reeves WH, Han K, Cha S. 2022. The inflammatory signature in monocytes of Sjogren's syndrome and systemic lupus erythematosus, revealed by the integrated Reactome and drug target analysis. Genes Genomics 44: 1215-1229.
Levanon EY, Eisenberg E, Yelin R, Nemzer S, Hallegger M, Shemesh R, Fligelman ZY, Shoshan A, Pollock SR, Sztybel D et al. 2004. Systematic identification of abundant A-to-I editing sites in the human transcriptome. Nat Biotechnol 22: 1001-1005.
Li Y, Ma C, Liao S, Qi S, Meng S, Cai W, Dai W, Cao R, Dong X, Kramer BK et al. 2022. Combined proteomics and single cell RNA-sequencing analysis to identify biomarkers of disease diagnosis and disease exacerbation for systemic lupus erythematosus. Front Immunol 13: 969509.
Liu CX, Li X, Nan F, Jiang S, Gao X, Guo SK, Xue W, Cui Y, Dong K, Ding H et al. 2019. Structure and Degradation of Circular RNAs Regulate PKR Activation in Innate Immunity. Cell 177: 865-880 e821.
Love MI, Huber W, Anders S. 2014. Moderated estimation of fold change and dispersion for RNA-seq data with DESeq2. Genome Biol 15: 550.
Matoba Y, Abiko C, Ikeda T, Aoki Y, Suzuki Y, Yahagi K, Matsuzaki Y, Itagaki T, Katsushima F, Katsushima Y, Mizuta K. 2015. Detection of the human coronavirus 229E, HKU1, NL63, and OC43 between 2010 and 2013 in Yamagata, Japan. Jpn J Infect Dis 68: 138-141.
Miller B, Silverstein A, Flores M, Cao K, Kumagai H, Mehta HH, Yen K, Kim SJ, Cohen P. 2021. Host mitochondrial transcriptome response to SARS-CoV-2 in multiple cell models and clinical samples. Sci Rep 11: 3.
Minkoff JM, tenOever B. 2023. Innate immune evasion strategies of SARS-CoV-2. Nat Rev Microbiol 21: 178-194.
Murphy WI, Attardi B, Tu C, Attardi G. 1975. Evidence for complete symmetrical transcription in vivo of mitochondrial DNA in HeLa cells. J Mol Biol 99: 809-814.
Nagaike T, Suzuki T, Katoh T, Ueda T. 2005. Human mitochondrial mRNAs are stabilized with polyadenylation regulated by mitochondria-specific poly(A) polymerase and polynucleotide phosphorylase. J Biol Chem 280: 19721-19727.
Nandula SR, Scindia YM, Dey P, Bagavant H, Deshmukh US. 2011. Activation of innate immunity accelerates sialoadenitis in a mouse model for Sjogren's syndrome-like disease. Oral Dis 17: 801-807.
Ojala D, Montoya J, Attardi G. 1981. tRNA punctuation model of RNA processing in human mitochondria. Nature 290: 470-474.
Pan L, Lu MP, Wang JH, Xu M, Yang SR. 2020. Immunological pathogenesis and treatment of systemic lupus erythematosus. World J Pediatr 16: 19-30.

Peisley A, Hur S. 2013. Multi-level regulation of cellular recognition of viral dsRNA. Cell Mol Life Sci 70: 1949-1963.
Peng Z, Cheng Y, Tan BC, Kang L, Tian Z, Zhu Y, Zhang W, Liang Y, Hu X, Tan X et al. 2012. Comprehensive analysis of RNA-Seq data reveals extensive RNA editing in a human transcriptome. Nat Biotechnol 30: 253-260.
Quin J, Sedmik J, Vukic D, Khan A, Keegan LP, O'Connell MA. 2021. ADAR RNA Modifications, the Epitranscriptome and Innate Immunity. Trends Biochem Sci 46: 758-771.
Rehwinkel J, Gack MU. 2020. RIG-I-like receptors: their regulation and roles in RNA sensing. Nat Rev Immunol 20: 537-551.
Ronnblom L, Pascual V. 2008. The innate immune system in SLE: type I interferons and dendritic cells. Lupus 17: 394-399.
Ruzzenente B, Metodiev MD, Wredenberg A, Bratic A, Park CB, Camara Y, Milenkovic D, Zickermann V, Wibom R, Hultenby K et al. 2012. LRPPRC is necessary for polyadenylation and coordination of translation of mitochondrial mRNAs. EMBO J 31: 443-456.
Sasarman F, Brunel-Guitton C, Antonicka H, Wai T, Shoubridge EA, Consortium L. 2010. LRPPRC and SLIRP interact in a ribonucleoprotein complex that regulates posttranscriptional gene expression in mitochondria. Mol Biol Cell 21: 1315-1323.
Sayyed UMH, Mahalakshmi R. 2022. Mitochondrial protein translocation machinery: From TOM structural biogenesis to functional regulation. J Biol Chem 298: 101870.
Seth RB, Sun L, Ea CK, Chen ZJ. 2005. Identification and characterization of MAVS, a mitochondrial antiviral signaling protein that activates NF-kappaB and IRF 3. Cell 122: 669-682.
Shao H, Lan D, Duan Z, Liu Z, Min J, Zhang L, Huang J, Su J, Chen S, Xu A. 2006. Upregulation of mitochondrial gene expression in PBMC from convalescent SARS patients. J Clin Immunol 26: 546-554.
Shimizu T, Nakamura H, Kawakami A. 2021. Role of the Innate Immunity Signaling Pathway in the Pathogenesis of Sjogren's Syndrome. Int J Mol Sci 22.
Stewart H, Lu Y, O'Keefe S, Valpadashi A, Cruz-Zaragoza LD, Michel HA, Nguyen SK, Carnell GW, Lukhovitskaya N, Milligan R et al. 2023. The SARS-CoV-2 protein ORF3c is a mitochondrial modulator of innate immunity. iScience 26: 108080.
Su J, Liu D, Yang F, Zuo MQ, Li C, Dong MQ, Sun S, Sui SF. 2022a. Structural basis of Tom20 and Tom22 cytosolic domains as the human TOM complex receptors. Proc Natl Acad Sci U S A 119: e2200158119.
Su X, Pillai S, Liu Y, Tran SD. 2022b. Isolation, Culture, and Characterization of Primary Salivary Gland Cells. Curr Protoc 2: e479.
Szczesny RJ, Borowski LS, Brzezniak LK, Dmochowska A, Gewartowski K, Bartnik E, Stepien PP. 2010. Human mitochondrial RNA turnover caught in flagranti: involvement of hSuv3p helicase in RNA surveillance. Nucleic Acids Res 38: 279-298.
Szewczyk M, Malik D, Borowski LS, Czarnomska SD, Kotrys AV, Klosowska-Kosicka K, Nowotny M, Szczesny RJ. 2020. Human REXO2 controls short mitochondrial RNAs generated by mtRNA processing and decay machinery to prevent accumulation of double-stranded RNA. Nucleic Acids Res 48: 5572-5590.
van de Sandt CE, Kreijtz JH, Rimmelzwaan GF. 2012. Evasion of influenza A viruses from innate and adaptive immune responses. Viruses 4: 1438-1476.

Wang G, Chen HW, Oktay Y, Zhang J, Allen EL, Smith GM, Fan KC, Hong JS, French SW, McCaffery JM et al. 2010. PNPASE regulates RNA import into mitochondria. Cell 142: 456-467.
Weber F, Wagner V, Rasmussen SB, Hartmann R, Paludan SR. 2006. Double-stranded RNA is produced by positive-strand RNA viruses and DNA viruses but not in detectable amounts by negative-strand RNA viruses. J Virol 80: 5059-5064.
White MJ, McArthur K, Metcalf D, Lane RM, Cambier JC, Herold MJ, van Delft MF, Bedoui S, Lessene G, Ritchie ME et al. 2014. Apoptotic caspases suppress mtDNA-induced STING-mediated type I IFN production. Cell 159: 1549-1562.
Wiedemann N, Pfanner N. 2017. Mitochondrial Machineries for Protein Import and Assembly. Annu Rev Biochem 86: 685-714.
Yamano K, Yatsukawa Y, Esaki M, Hobbs AE, Jensen RE, Endo T. 2008. Tom20 and Tom22 share the common signal recognition pathway in mitochondrial protein import. J Biol Chem 283: 3799-3807.
Yoon J, Ku D, Lee M, Lee N, Im SG, Kim Y. 2023. Resveratrol Attenuates the Mitochondrial RNA-Mediated Cellular Response to Immunogenic Stress. Int J Mol Sci 24.
Yoon J, Lee M, Ali AA, Oh YR, Choi YS, Kim S, Lee N, Jang SG, Park S, Chung JH et al. 2022. Mitochondrial double-stranded RNAs as a pivotal mediator in the pathogenesis of Sjögren's syndrome. Mol Ther Nucleic Acids 30: 257-269.
Youle RJ, Strasser A. 2008. The BCL-2 protein family: opposing activities that mediate cell death. Nat Rev Mol Cell Biol 9: 47-59.
Young PG, Attardi G. 1975. Characterization of double-stranded RNA from HeLa cell mitochondria. Biochem Biophys Res Commun 65: 1201-1207.
Zheng X, Bevilacqua PC. 2004. Activation of the protein kinase PKR by short double-stranded RNAs with single-stranded tails. RNA 10: 1934-1945.

FIGURES

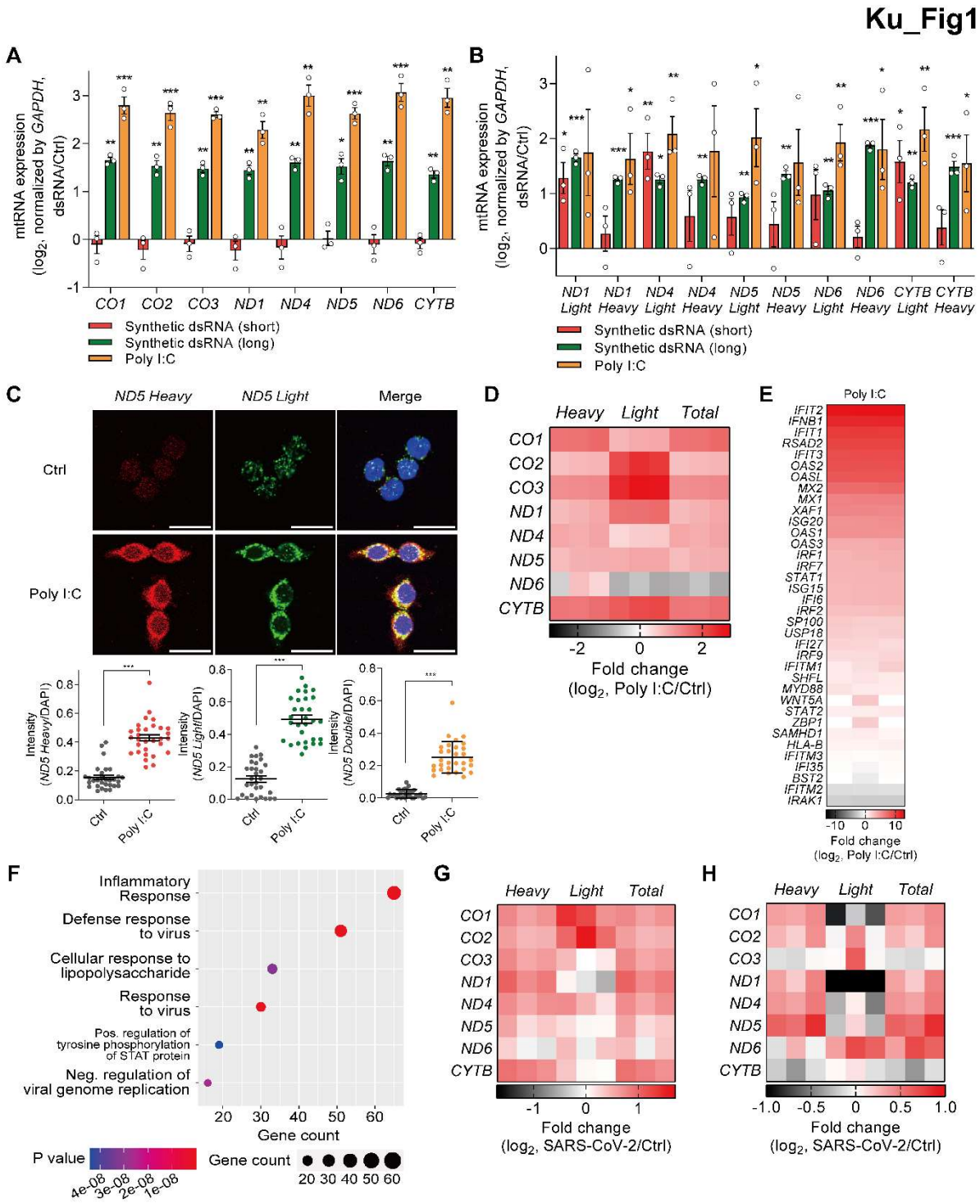

Figure 1. Antiviral response to long exogenous dsRNAs upregulate mtRNA expression. (A, B) Analysis of total (A) and strand-specific (B) mtRNA expression upon introduction of dsRNAs with different lengths in HCT116 cells. (C) smRNA-FISH analysis for the individual strand of *ND5* mtRNAs in poly I:C transfected cells. Nuclei were stained using DAPI.

Quantified signal intensities calculated by taking an average of over 30 images are presented below. Scale bar, 25 μm. (D, E) Heatmap of $\log_2$ fold changes for the two strands of mtRNAs (D) and type I IFN genes (E) upon poly I:C transfection. The three columns represent biological replicates. (F) The GO analysis of DEGs of poly I:C-transfected cells. Genes with $\log_2$ fold change over 2 and p-value less than 0.05 were analyzed. (G, H) Heatmap of fold change for the two strands of mtRNAs upon SARS-CoV-2 infection in A549-ACE2 (G) and Calu3 (H). Previously published RNA-seq data were reanalyzed (Miller et al. 2021). Unless mentioned, three independent experiments were carried out, and error bars denote s.e.m. All of the statistical significances were calculated using one-tail Student's t-tests; * $p \leq 0.05$, ** $p \leq 0.01$, and *** $p \leq 0.001$.

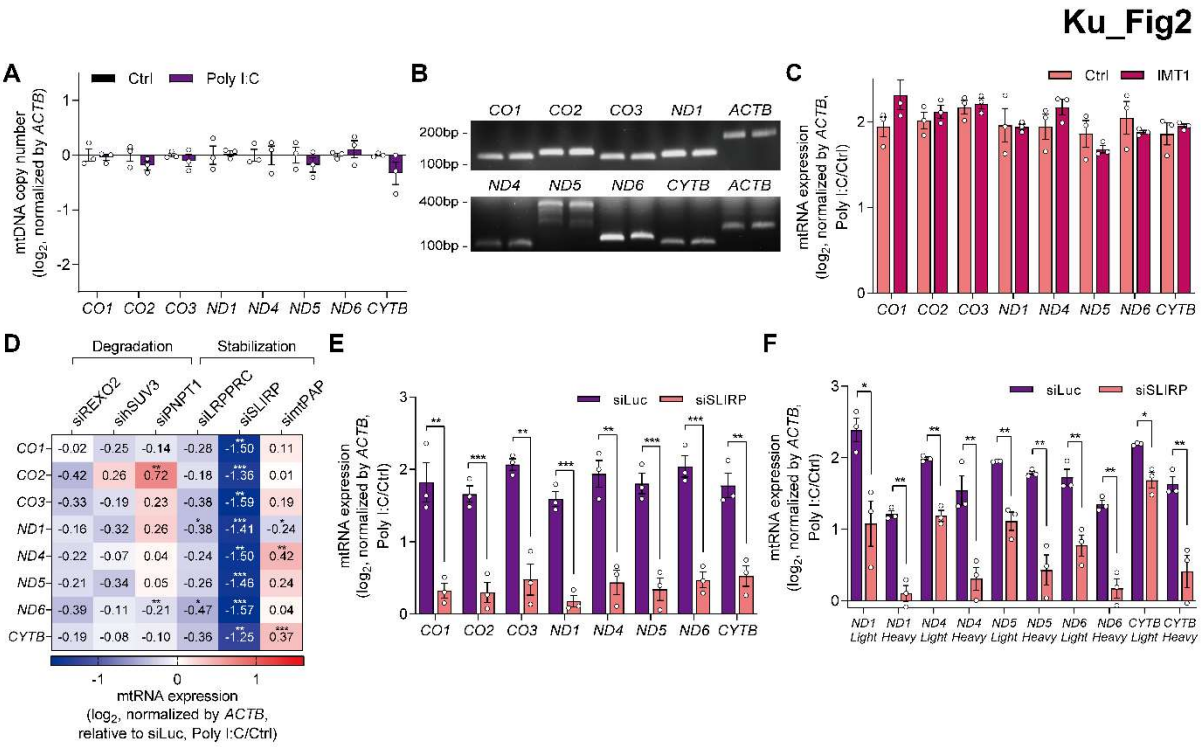

Figure 2. Stabilization by SLIRP results in mtRNA upregulation during antiviral response. (A) Analysis of mtDNA copy number upon poly I:C transfection in HCT116 cells. (B) Confirmation of the qPCR result by agarose gel electrophoresis to detect mtDNA amplicon. (C) Normalized total mtRNA levels upon poly I:C transfection 48 h after IMT1 treatment. Data are normalized only to those of DEPC-transfected cells in order to analyze the degree of mtRNA induction by poly I:C. (D) Heatmap of the degree of mtRNA induction upon poly I:C transfection in cells transfected with the indicated siRNAs. (E, F) Analysis of total (E) and strand-specific (F) mtRNAs in control and SLIRP knocked down HCT116 cells. Three independent experiments were carried out, and error bars denote s.e.m. All of the statistical significances were calculated using one-tail Student's t-tests; * $p \leq 0.05$, ** $p \leq 0.01$, and *** $p \leq 0.001$.

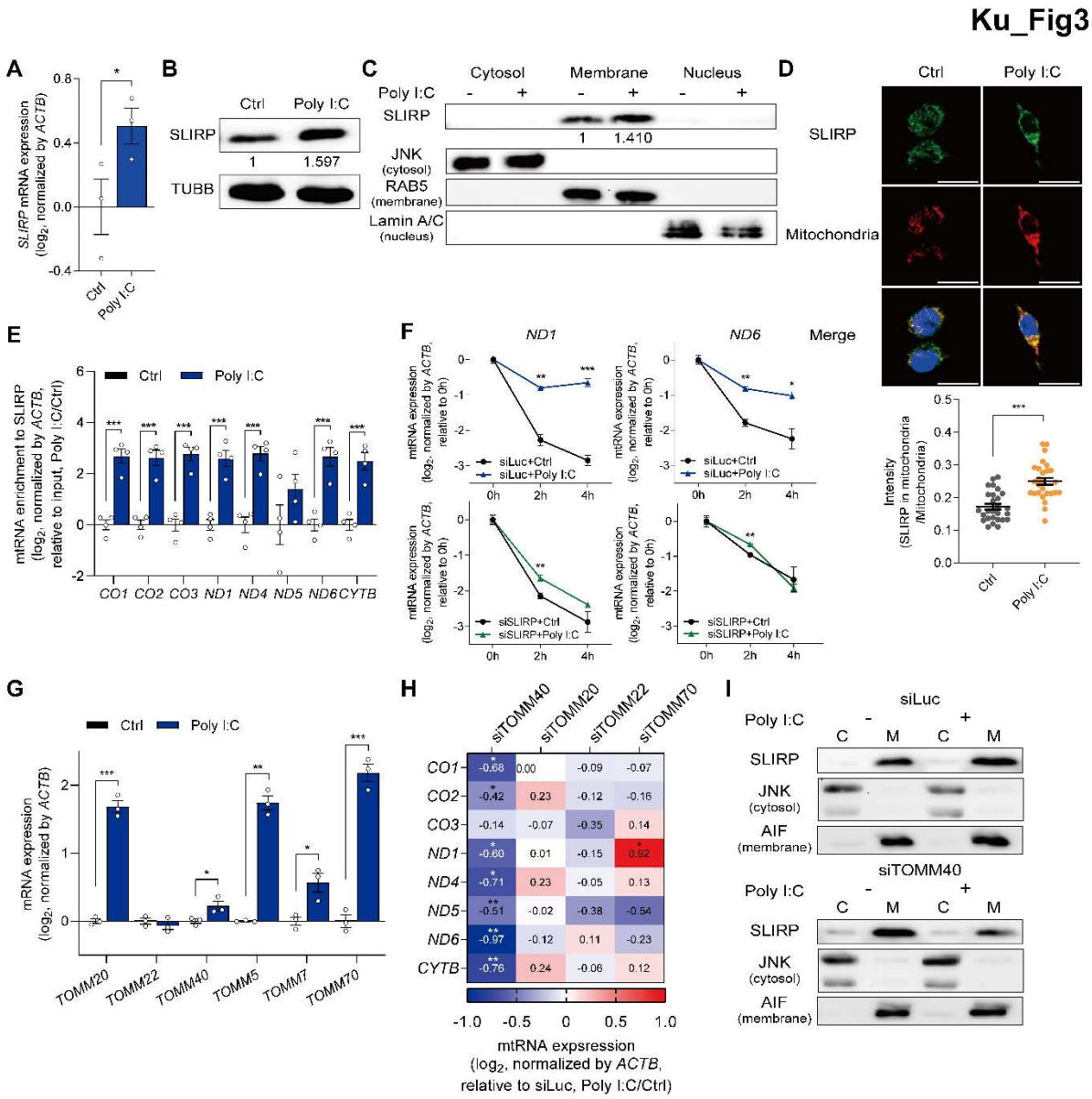

Figure 3. SLIRP expression and its mitochondrial import are upregulated during antiviral response. (A, B) Analysis of *SLIRP* mRNA (A) and protein (B) expression in HCT116 cells transfected with poly I:C. (C) The expression of SLIRP in free cytosol, membrane organelle, and nucleus. The following proteins are used to confirm successful subcellular fractionation: JNK for the free cytosol, RAB5 for the membrane, and Lamin A/C for the nucleus. (D) Representative fluorescence images of SLIRP and mitochondria upon poly I:C transfection. Scale bar, 25 μm. Quantified signal intensities averaged over 17 images are presented below. (E) Interaction between SLIRP and mtRNAs upon poly I:C transfection was examined by SLIRP fCLIP followed by RT-qPCR analysis (n=4). (F) Analysis of mtRNA stability before and after poly I:C transfection in control and SLIRP-deficient cells. (G)

Analysis of the RNA expression of genes involved in the TOM complex upon poly I:C stimulation. (H) Heatmap showing the degree of mtRNA induction by poly I:C after downregulating the indicated target genes involved in the TOM complex. (I) Western blot analysis for SLIRP expression upon poly I:C in the cytosol and membrane fraction, with or without TOMM40. JNK is used as a marker for the cytosol fraction while AIF is used as a marker for the membrane fraction. Unless mentioned, three independent experiments were carried out, and error bars denote s.e.m. All of the statistical significances were calculated using one-tail Student's t-tests; * $p \leq 0.05$, ** $p \leq 0.01$, and *** $p \leq 0.001$.

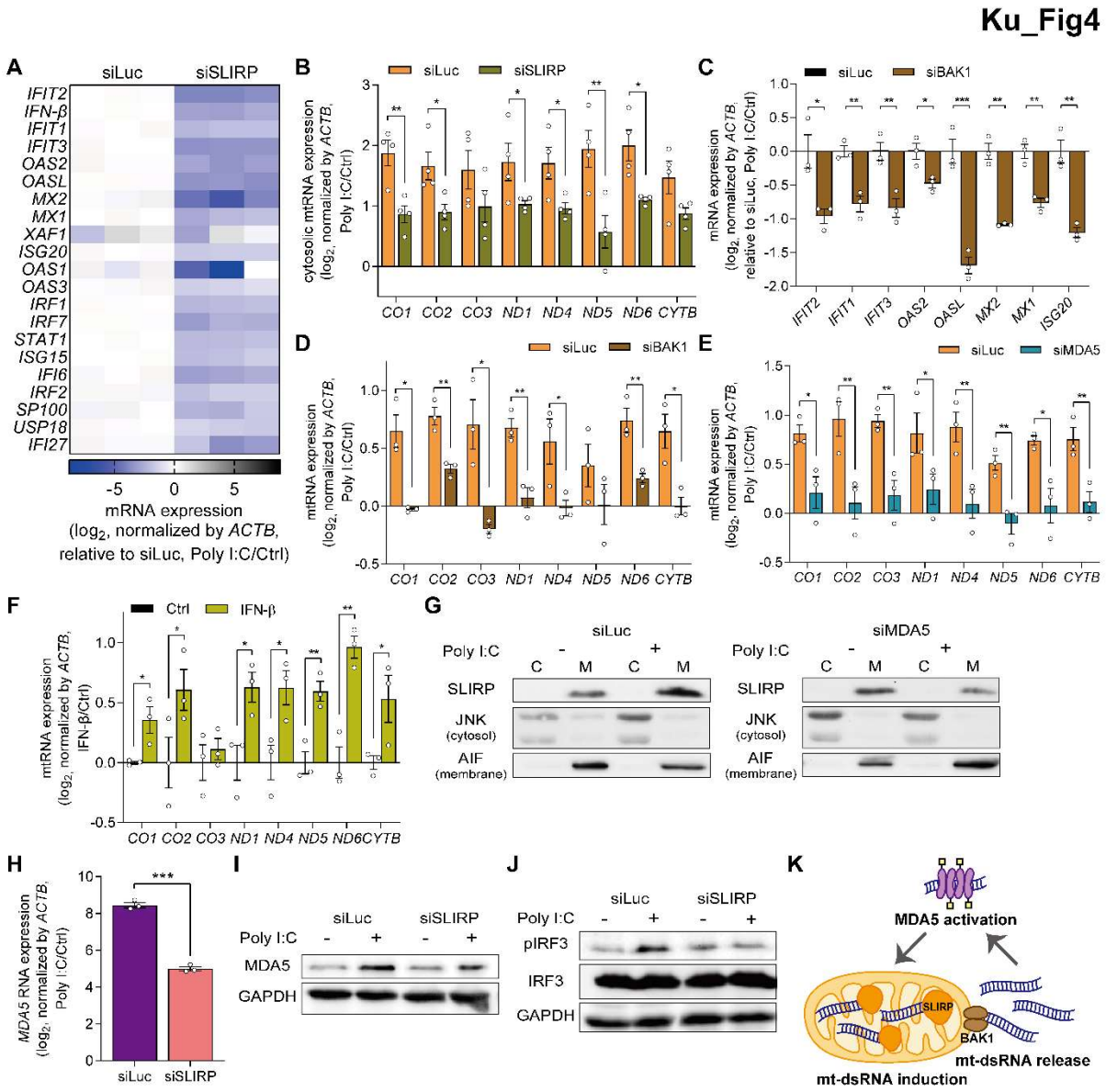

Figure 4. Antiviral signaling is amplified via the MDA5-mtRNA-SLIRP positive feedback loop. (A) Heatmap of log2 fold change of type I IFN genes upon poly I:C transfection in control and SLIRP-deficient cells. The three columns represent biological replicates. (B) Cytosolic mtRNA expression in poly I:C transfected cells with or without SLIRP (n=4). (C, D) The effect of BAK1 downregulation on the ISG (C) and mtRNA (D) induction by poly I:C. (E) Analysis of mtRNA expression upon poly I:C transfection with or without MDA5. (F) The mtRNA expression upon IFN-β treatment. (G) Western blot analysis for SLIRP localization upon poly I:C with or without MDA5. JNK is used as a marker for the cytosol fraction while AIF is used as a marker for the membrane fraction. (H, I) The expression of *MDA5* mRNA (H) and protein (I) expression after poly I:C transfection in cells deficient in SLIRP. (J) The effect of SLIRP downregulation on the IRF3 phosphorylation upon poly I:C. (K) A model for the positive

feedback amplification of antiviral signaling consists of mtRNA induction, cytosolic release, and MDA5 activation. Unless mentioned, three independent experiments were carried out, and error bars denote s.e.m. All of the statistical significances were calculated using one-tail Student's t-tests; * $p \leq 0.05$, ** $p \leq 0.01$, and *** $p \leq 0.001$.

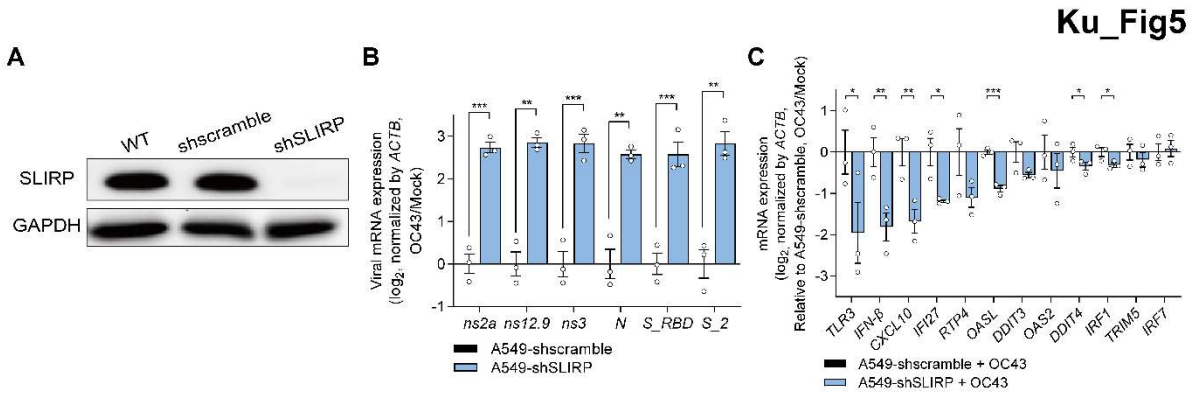

Figure 5. SLIRP downregulation enhances OC43 infection and attenuates ISG induction. (A) Western blot analysis of SLIRP expression in A549 cells transduced with shSLIRP. (B, C) Analysis of viral mRNA expression (B) and ISG induction (C) after infecting SLIRP-deficient cells with OC43 at MOI = 1. N=3 and error bars denote s.e.m. All of the statistical significances were calculated using one-tail Student's t-tests; * $p \leq 0.05$, ** $p \leq 0.01$, and *** $p \leq 0.001$.

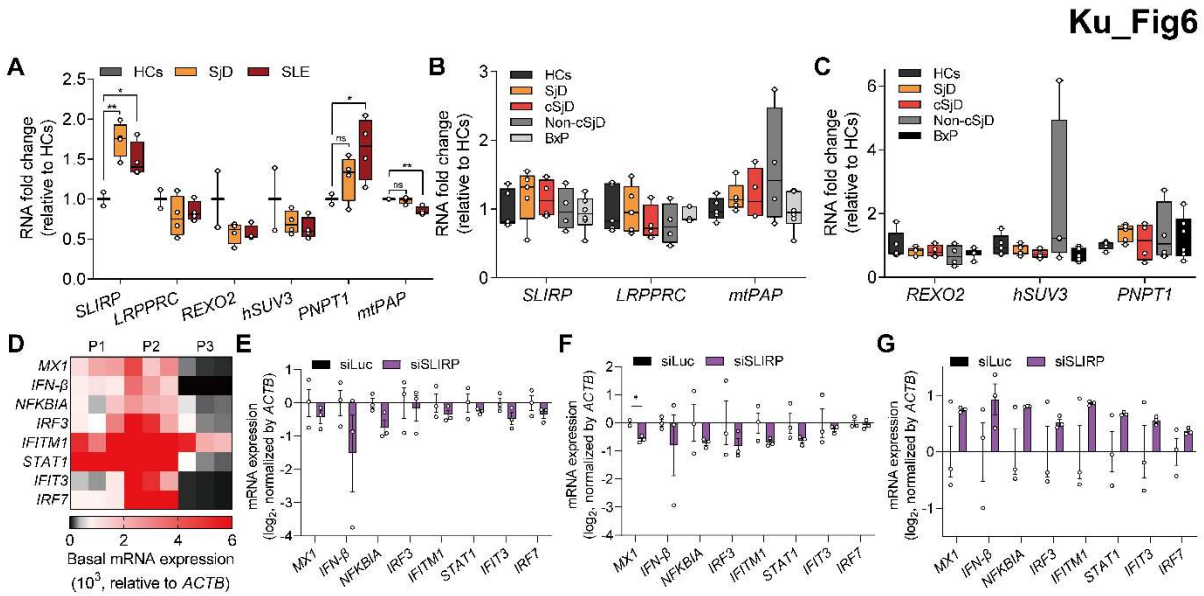

Figure 6. SLIRP is associated with the immune signature of SjD and SLE patients. (A) Analysis of gene expression related to mtRNA stability in monocytes of HCs (n=2), SjD (n=4), and SLE (n=4) patients. (B, C) Analysis of gene expression related to mtRNA stability in monocytes of HCs (n=5), SjD (n=5), cSjD (n=4), Non-cSjD (n=4), and BxP (n=6). (D) The heatmap representing the unstimulated expression of selected ISGs in primary minor salivary gland cells isolated from three SjD patients. The three columns represent three biological replicates. (E-G) Analysis of ISG expression after knockdown of SLIRP in primary minor salivary gland cells of three patients from (D). Unless mentioned, n=3 and error bars denote s.e.m for all except for the organoid data. All of the statistical significances were calculated using one-tail Student's t-tests; * $p \leq 0.05$, ** $p \leq 0.01$, and *** $p \leq 0.001$.